


第2回マツモト技術講演会 平成19年11月26日

チタンおよびジルコニウムアルコキシド 誘導体の合成と性質




郡司天博・阿部芳首

東京理科大学 理工学部 工業化学科
〒278-8510 千葉県野田市山崎2641
電話 04-7122-9499 fax 04-7123-9890
e-mail gunji@rs.noda.tus.ac.jp

 Tokyo University of Science

講演内容

1. アルコキシシランとチタン, ジルコニウムアルコキシド
2. チタナシロキサン, ジルコナシロキサン化合物
3. ポリジルコナシロキサン
4. ポリジルコノキサン

 Tokyo University of Science



$M(\text{OEt})_4$ における金属の部分正電荷 $\delta(M)$ ¹⁾

Si	+0.32	<ul style="list-style-type: none"> ・ Ti, ZrはSiより正電荷が大きい。 ・ TiとZrの正電荷は同程度。
Ti	+0.63	
Zr	+0.65	

pH7における $M(\text{OEt})_4$ の加水分解速度定数 ¹⁾

Si	5×10^{-9} l/mol/s	<ul style="list-style-type: none"> ・ TiはSiより加水分解速度が大きい。
Ti	1×10^{-3} l/mol/s	

安定な配位数

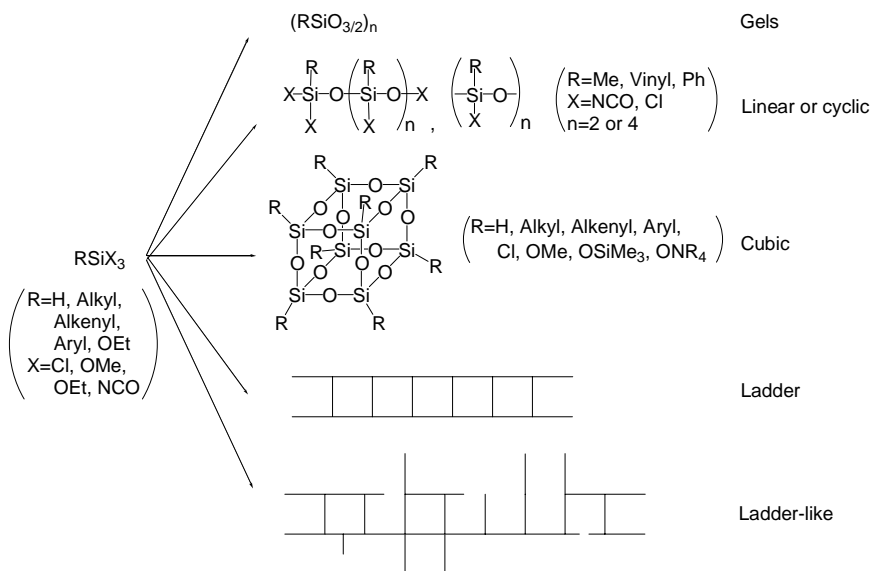
Si	4	<ul style="list-style-type: none"> ・ Ti, ZrはSiより多配位が可能。
Ti	4, 6	
Zr	4, 6, 8	

1) J. D. Wright and N. A. J. M. Sommerdijk, "Sol-Gel Materials Chemistry and Applications", Golden and Breach Science Publishers, pp. 53-54.

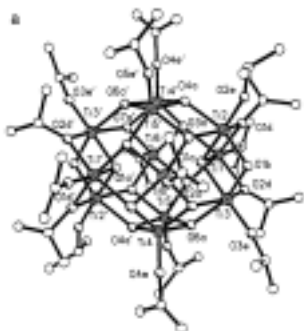
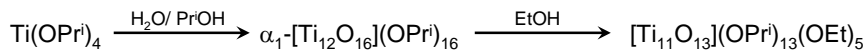
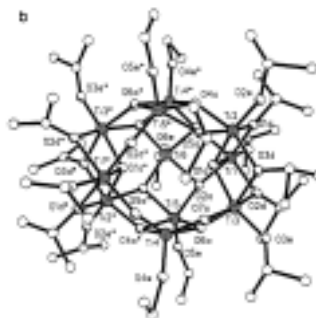
金属アルコキシドなどの構造

構造式			
組成式	$\text{Si}(\text{OEt})_4$	$\text{Ti}(\text{OPr}^i)_4$	$\text{Zr}(\text{OPr}^i)_4$
金属の配位数	4	4	4
構造式			
組成式	$\text{Zr}(\text{OPr}^i)_4 \cdot \text{Pr}^i\text{OH}$	$\text{Zr}(\text{OH})_8 \cdot (\text{H}_2\text{O})_{16}$	
金属の配位数	6	8	

アルコキシシランの加水分解重縮合反応

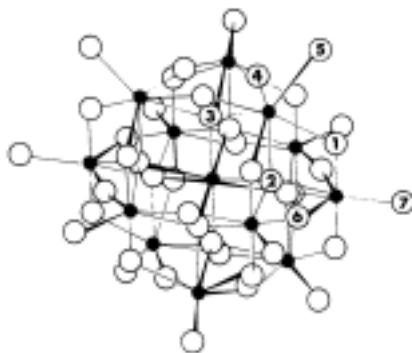
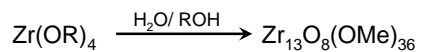


チタンアルコキシドの加水分解重縮合反応


 $\alpha_1\text{-}[\text{Ti}_{12}\text{O}_{16}](\text{OPri})_{16}$

 $[\text{Ti}_{11}\text{O}_{13}](\text{OPri})_{13}(\text{OEt})_5$

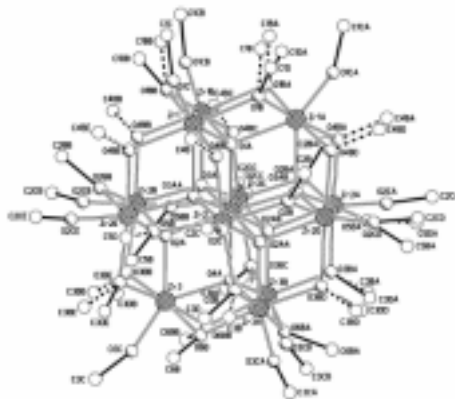
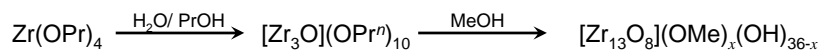
V. W. Day, T. A. Eberspacher, W. G. Klemperer, and C. W. Park, *J. Am. Chem. Soc.*, **1993**, *115*, 8469-8410.

ジルコニウムアルコキシドの加水分解重縮合反応


 $\text{Zr}_{13}\text{O}_8(\text{OCH}_3)_{36}$

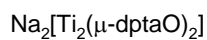
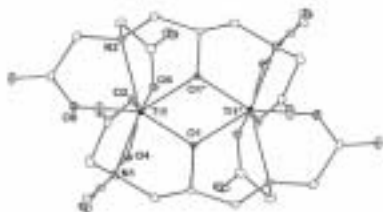
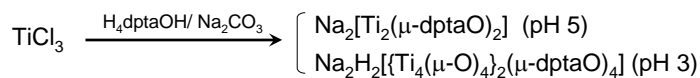
B. Morosin, *Acta Cryst.*, **1977**, *B33*, 303-305.

ジルコニウムアルコキシドの加水分解重縮合反応

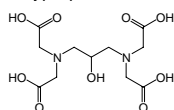


V. W. Day, W. G. Klemperer, and M. M. Pafford, *Inorg. Chem.*, **2005**, *44*, 5397-5404.

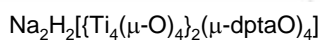
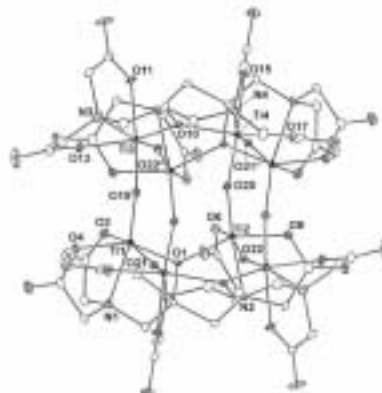
キューブチタン化合物の合成 (1)



2-hydroxypropane-1,3-diamine-*N,N,N',N'*-tetraacetic acid

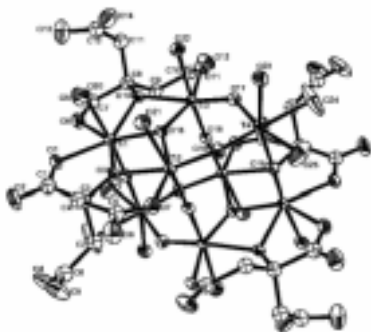
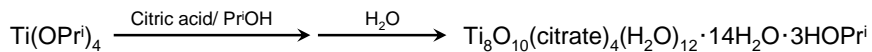


(H₄dptaOH)

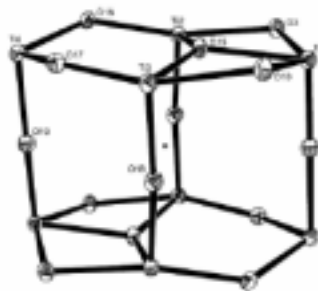


Y. Miyashita, Md. M. Islam, N. Amir, K. Fujisawa, and K. Okamoto, *Chem. Lett.*, **2004**, *33*, 1516-1517.

キューブチタン化合物の合成 (2)



$\text{Ti}_8\text{O}_{10}(\text{citrate})_4(\text{H}_2\text{O})_{12} \cdot 14\text{H}_2\text{O} \cdot 3\text{HOPri}$

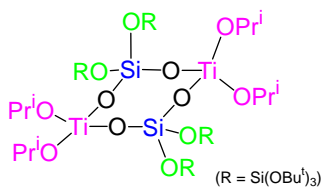


Ti_8O_{14} cage structure

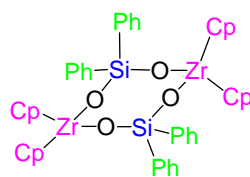
T. Kemmitt, N. I. Al-Salim, G. J. Gainsford, A. Bubendorfer, and M. Waterland, *Inorg. Chem.*, **2004**, 43, 6300-6306.

講演内容

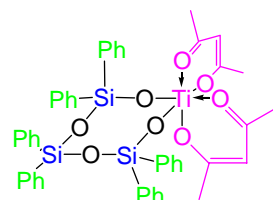
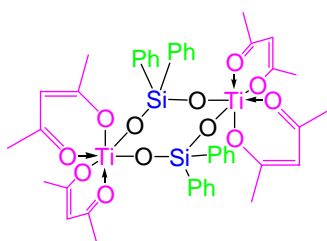
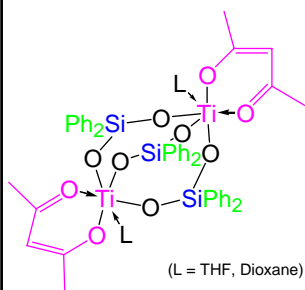
1. アルコキシシランとチタン, ジルコニウムアルコキシド
2. チタナシロキサン, ジルコナシロキサン化合物
3. ポリジルコナシロキサン
4. ポリジルコノキサン



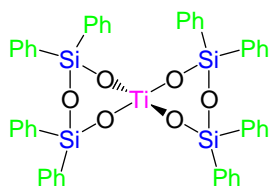
Y. Abe and I. Kijima, *Bull. Chem. Soc. Jpn.*, **43**, 466 (1970)



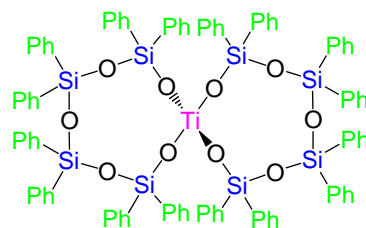
J. F. Harrod, et al., *Inorg. Chem.*, **33**, 1292 (1994)



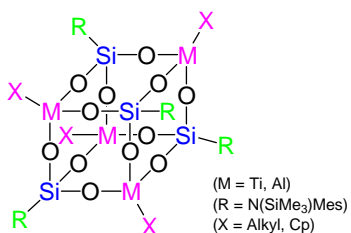
D. Hoebbel, et al., *J. Mater. Chem.*, **8**, 171-8 (1998)



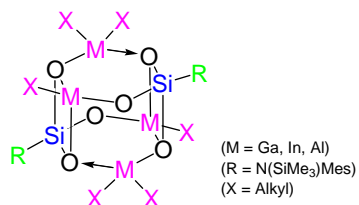
K. A. Andrianov, et al., *Zh. Obshch. Khim.*, **46**, 1533 (1976);
K. A. Andrianov, et al., *Izv. Akad. Nauk SSSR Ser. Khim.*, **10**, 2314 (1977).

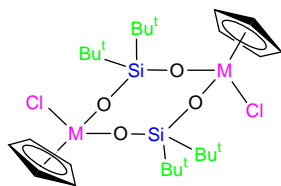


M. B. Hursthouse and M. A. Hossain, *Polyhedron*, **3**, 95 (1984)

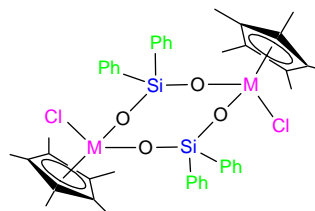


R. Murugavel, V. Chandrasekhar, H. W. Roesky, *Acc. Chem. Res.*, **29**, 183-9 (1996).

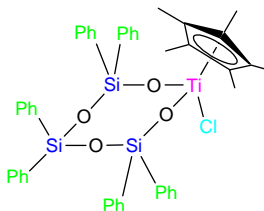




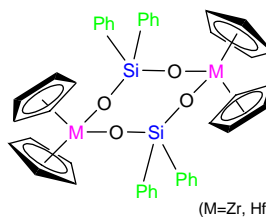
F. Q. Liu, H. G. Schmidt, M. Noltemeyer, C. Freire-Erdbruegger, G. M. Sheldrick, H. W. Roesky, *Zeit. Natur., B: Chem. Sci.*, **47**, 1085-90 (1992).



F. Q. Liu, H. G. Schmidt, M. Noltemeyer, C. Freire-Erdbruegger, G. M. Sheldrick, H. W. Roesky, *Zeit. Natur., B: Chem. Sci.*, **47**, 1085-90 (1992).

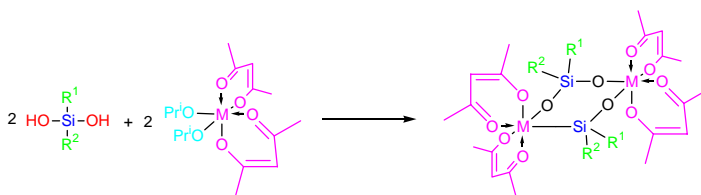


R. Murugavel, V. S. Shete, K. Baheti, P. Davis, *J. Organometal. Chem.*, **625**, 195-199 (2001).



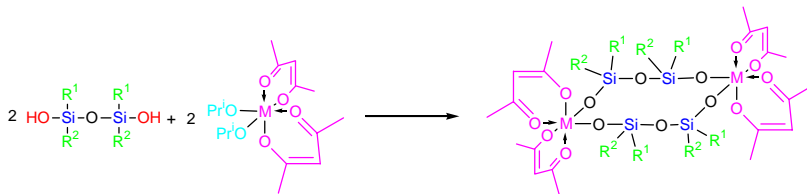
(M=Zr, Hf)

J. F. Harrod, et. al., *Inorg. Chem.*, **33**, 1292 (1994)



R¹=R²=OBu^t, M=Ti: Yield: 85 %. Mp: 188-192 °C (Decomp.). IR 1590 ($\nu_{C=O}$), 1530 ($\nu_{C=C}$), 1000 (ν_{Si-O-C}), 960 ($\nu_{Si-O-Ti}$) (cm^{-1}); ¹H NMR δ =1.3 (9H, t, -OBu^t), 2.0 (6H, d, C-CH₃), 5.5 (1H, s, -CH=); ¹³C NMR δ =25.3 (CH₃CO-), 26.8 (CH₃CO-), 31.6 ((CH₃)₂CO-), 71.7 ((CH₃)₂CO-), 103.8 (-CH=), 185.9 (CH₃CO-), 191.8 (CH₃CO-); ²⁹Si NMR δ =-107.8. 元素分析値: Found: Si, 6.1; Ti, 10.5 %. Calcd for C₃₆H₆₄O₁₆Si₂Ti₂: Si, 6.2; Ti, 10.6 %.

R¹=R²=OBu^t, M=Zr: Yield: 97 %. Mp: 197-198 °C (Decomposition). IR 1590 ($\nu_{C=O}$), 1530 ($\nu_{C=C}$), 1010 (ν_{Si-O-C}), 970 ($\nu_{Si-O-Zr}$) (cm^{-1}); ¹H NMR δ =1.3 (9H, s, -OBu^t), 2.0 (6H, s, C-CH₃), 5.6 (1H, s, -CH=); ¹³C NMR δ =26.5 (CH₃CO-), 31.5 ((CH₃)₂CO-), 71.0 ((CH₃)₂CO-), 104.0 (-CH=), 190.8 (CH₃CO-); ²⁹Si NMR δ =-102.3. Found: Si, 5.6; Zr, 18.4 %. 元素分析値: Calcd for C₃₆H₆₄O₁₆Si₂Zr: Si, 5.7; Zr, 18.4 %.



R¹=Me, R²=OBu^t, M=Ti: Yield: 82.1%. Mp 162.4 (Decomp.). IR 2970, 1590, 1530, 1280, 1020, 1050, 990, 970 (cm⁻¹); ¹H NMR (400 MHz) δ= 0.10 (s, 12H), 1.28 (s, 36H), 2.00 (s, 24H), 5.60 (s, 4H); ¹³C NMR (100.6 MHz) δ= -2.64 (s), 25.4 (s), 26.9 (s), 31.6 (s), 72.7 (s), 104.4 (s), 186.5 (s), 192.7 (s); ²⁹Si NMR (79.5 MHz) δ= -55.7 (s). MS *m/z* 1052 (M⁺). Found: Si, 10.5%. Calcd. for C₄₀H₇₂O₁₈Si₄Ti₂; Si, 10.6%.

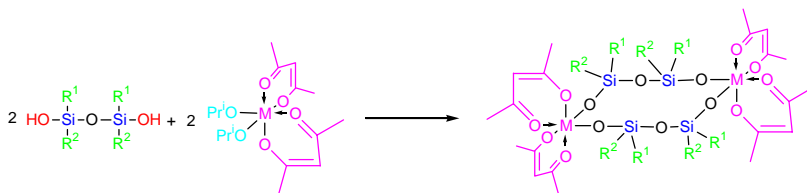
R¹=R²=OBu^t, M=Ti: Yield: 81.9%. Mp 126.3 (Decomp.). IR 2970, 1580, 1530, 1070, 1020, 960 (cm⁻¹); ¹H NMR (400 MHz) δ= 1.31 (s, 72H), 1.99 (s, 24H), 5.63 (s, 4H); ¹³C NMR (100.6 MHz) δ= 25.4 (s), 26.8 (s), 31.3 (s), 72.5 (s), 104.3 (s), 187.6 (s), 192.3 (s); ²⁹Si NMR (79.5 MHz) δ= -96.6 (s). MS *m/z* 1211 (M⁺-73). Found: Si, 8.5%. Calcd. for C₅₂H₁₀₀O₂₂Si₄Ti₂; Si, 8.5%.

R¹=OBu^t, R²=OPrⁱ, M=Ti: Yield: 72.3%. Mp 167.0-169.8 (Decomp.). IR 2977, 1708, 1592, 1106, 1070, 970 (cm⁻¹); ¹H NMR (400 MHz) δ= 1.22 (s, 24H), 1.34 (s, 36H), 1.99 (s, 24H), 4.29 (s, 4H), 5.99 (s, 4H); ¹³C NMR (100.6 MHz) δ= 23.9 (s), 25.4 (s), 26.8 (s), 31.6 (s), 65.9 (s), 74.6 (s), 104.7 (s), 187.9 (s), 192.6 (s); ²⁹Si NMR (79.5 MHz) δ= -92.5 (s). VPO *Mn* 1290. Found: Si, 9.2%. Calcd. for C₄₈H₉₂O₂₂Si₄Ti₂; Si, 9.2%.

R¹=Me, R²=OBu^t, M=Zr: Yield: 78.1%. Mp 159.5 (Decomp.). IR 2970, 1590, 1530, 1280, 1010, 1040, 990, 950 (cm⁻¹); ¹H NMR (400 MHz) δ= 0.09 (s, 12H), 1.29 (s, 36H), 1.96 (s, 24H), 5.61 (s, 4H); ¹³C NMR (100.6 MHz) δ= -2.64 (s), 26.9 (s), 31.5 (s), 72.7 (s), 104.4 (s), 190.9 (s); ²⁹Si NMR (79.5 MHz) δ= -64.9 (s). MS *m/z* 1123 (M⁺-15). Found: Si, 9.8%. Calcd. for C₄₀H₇₂O₁₈Si₄Zr₂; Si, 9.8%.

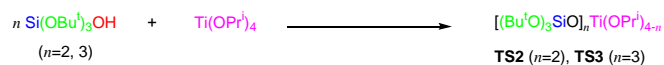
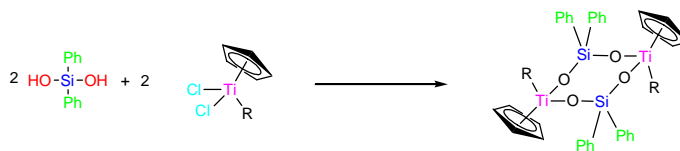
R¹=R²=OBu^t, M=Zr: Yield: 85.5%. Mp 132.5 (Decomp.). IR 2970, 1600, 1530, 1070, 1020, 920 (cm⁻¹); ¹H NMR (400 MHz) δ= 1.32 (s, 72H), 1.99 (s, 24H), 5.50 (s, 4H); ¹³C NMR (100.6 MHz) δ= 26.7 (s), 31.5 (s), 71.5 (s), 102.9 (s), 189.6 (s); ²⁹Si NMR (79.5 MHz) δ= -102.8 (s). MS *m/z* 1297 (M⁺-73). Found: Si, 8.1%. Calcd. for C₅₂H₁₀₀O₂₂Si₄Zr₂; Si, 8.1%.

R¹=OBu^t, R²=OPrⁱ, M=Zr: Yield: 70.5%. Mp 178.3-180.0 (Decomp.). IR 2981, 1710, 1592, 1105, 970, 916 (cm⁻¹); ¹H NMR (400 MHz) δ= 1.21 (s, 24H), 1.34 (s, 36H), 1.97 (s, 24H), 4.31 (s, 4H), 5.98 (s, 1H); ¹³C NMR (100.6 MHz) δ= 25.6 (s), 26.6 (s), 31.6 (s), 65.8 (s), 73.9 (s), 104.4 (s), 190.2 (s); ²⁹Si NMR (79.5 MHz) δ= -101.0 (s). VPO *Mn* 1385. Found: Si, 8.4%. Calcd. for C₄₈H₉₂O₂₂Si₄Zr₂; Si, 8.5%.



R¹=R²=Ph, M=Ti: Yield: 85.2%. Mp 197.9 (Decomp.). IR 3060, 2970, 1580, 1530, 1130, 1015, 940 (cm⁻¹); ¹H NMR (400 MHz) δ= 1.84 (br, 24H), 5.61 (s, 4H), 7.25 (m, 40H); ¹³C NMR (100.6 MHz) δ= 24.9 (s), 25.8 (s), 103.9 (d), 134.9 (q), 186.8 (s), 191.4 (s); ²⁹Si NMR (79.5 MHz) δ= -37.9 (s). MS *m/z* 1273 (M⁺-43). Found: Si, 8.4%. Calcd. for C₆₈H₆₈O₁₄Si₄Ti₂; Si, 8.5%.

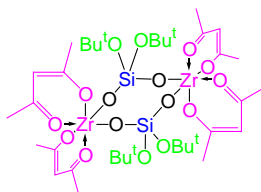
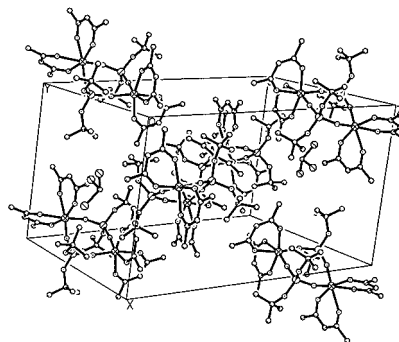
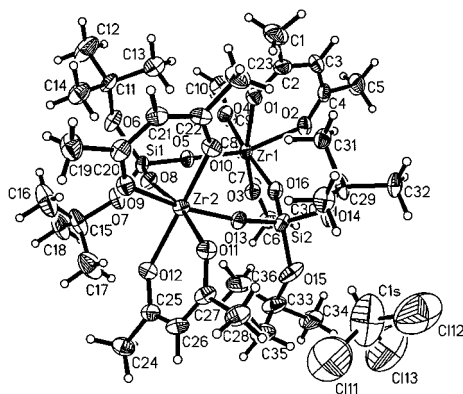
R¹=R²=Ph, M=Zr: Yield: 96.1%. Mp 211.7 (Decomp.). IR 3060, 2970, 1580, 1530, 1120, 1015, 930 (cm⁻¹); ¹H NMR (400 MHz) δ= 0.92-1.86 (m, 24H), 5.63 (t, 4H), 7.23 (m, 40H); ¹³C NMR (100.6 MHz) δ= 26.3 (s), 26.7 (s), 103.0 (d), 134.6 (q), 189.7 (s), 191.1 (s); ²⁹Si NMR (79.5 MHz) δ= -47.6 (s), -49.4 (s). MS *m/z* 1402 (M⁺). Found: Si, 7.9%. Calcd. for C₆₈H₆₈O₁₄Si₄Zr₂; Si, 8.0%.

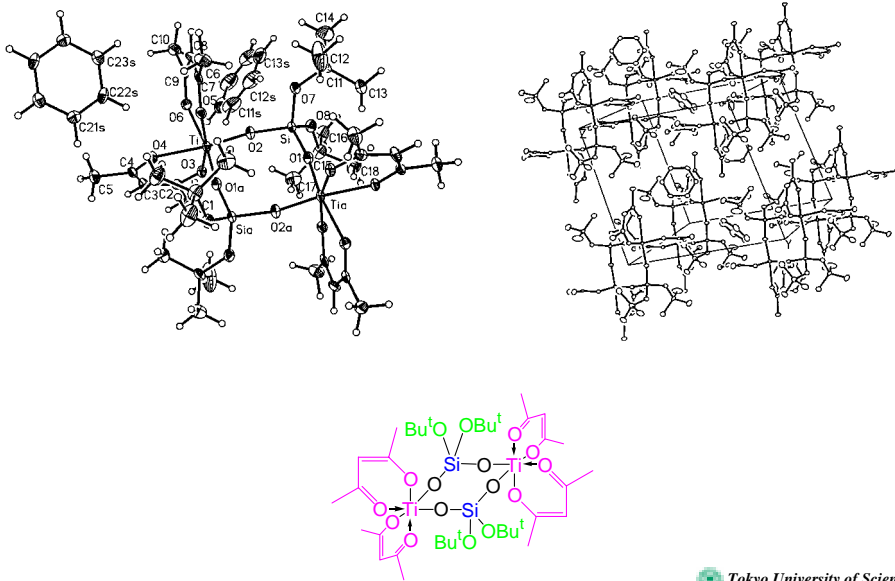


R=Cl (CTS-Cl): Yield: 88 %. Mp: 218 °C (Decomp.). IR 3067 ($\nu_{\text{C-H}}$), 1123 ($\nu_{\text{Si-C}}$), 942 ($\nu_{\text{Si-O-Ti}}$), 818 ($\nu_{\text{Ti-Cl}}$) (cm^{-1}); $^1\text{H NMR}$ δ =6.28 (s, 10H, Cp-H), 7.4-7.7 (m, 20H, Ar-H); $^{13}\text{C NMR}$ δ =118.3 (Ti-Cp), 128.1 (Si-Ph), 130.6 (Si-Ph), 134.1 (Si-Ph), 134.5 (Si-Ph); $^{29}\text{Si NMR}$ δ =-39.5.

R=Cp (CZS-Cp): CZS-Cp: Yield: 77 %. Mp: 182 °C (Decomp.). IR 3066 ($\nu_{\text{C-H}}$), 1118 ($\nu_{\text{Si-C}}$), 939 ($\nu_{\text{Si-O-Zr}}$) (cm^{-1}); $^1\text{H NMR}$ δ =6.09 (m, 20H, Cp-H), 7.2-7.7 (m, 20H, Ar-H); $^{13}\text{C NMR}$ δ =113.0 (Zr-Cp), 127.6 (Si-Ph), 128.3 (Si-Ph), 129.1 (Si-Ph), 134.4 (Si-Ph); $^{29}\text{Si NMR}$ δ =-44.8.

R=Cp (CTS-Cp): : Yield: 93 %. Mp: 168-170 °C (Decomp.). IR 3055 ($\nu_{\text{C-H}}$), 1428 ($\nu_{\text{C-C}}$), 1122 ($\nu_{\text{Si-C}}$), 947 ($\nu_{\text{Si-O-Ti}}$) (cm^{-1}); $^1\text{H NMR}$ δ =6.02-6.54 (m, 20H, Cp-H), 7.42-7.68 (m, 20H, Ar-H); $^{13}\text{C NMR}$ δ =118.8 (Ti-Cp), 119.4 (Ti-Cp), 128.1 (Si-Ph), 129.9 (Si-Ph), 135.3 (Si-Ph), 138.6 (Si-Ph); $^{29}\text{Si NMR}$ δ =-37.8.

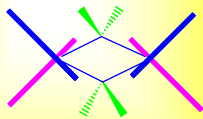




acac基の配置

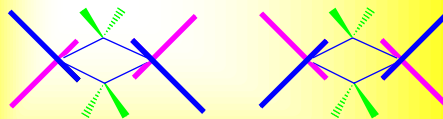
-CTSとCZSはacac基の配列が異なる-

CTS



acac基が直交

CZS



acac基は平行

CZSには2つの異性体が存在!

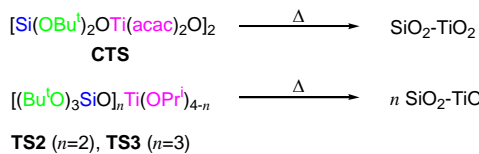
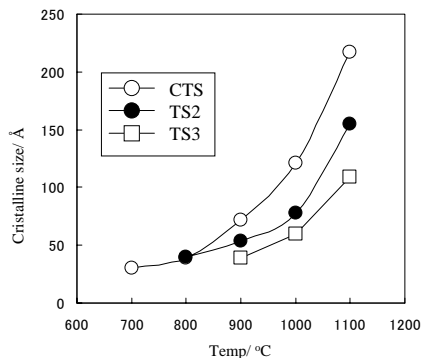


Table Crystal form^{a)} and the average crystallite size^{b)} of CTS, TS2, and TS3 on pyrolysis

Temp./ °C	CTS		TS2		TS3	
	Form	Size/ A	Form	Size/ A	Form	Size/ A
600	-	-	-	-	-	-
700	A	30	-	-	-	-
800	A	39	A	40	-	-
900	A	72	A	54	A	39
1000	A+R	121	A	78	A	60
1100	A+R	217	A+R	155	A	109

a) -: Amorphous, A: Anatase, R: Rutile b) Calculated from the Scherrer's equation.



Crystal size of TiO₂ anatase on heat-treatment

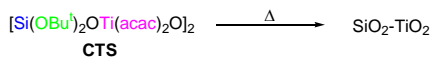
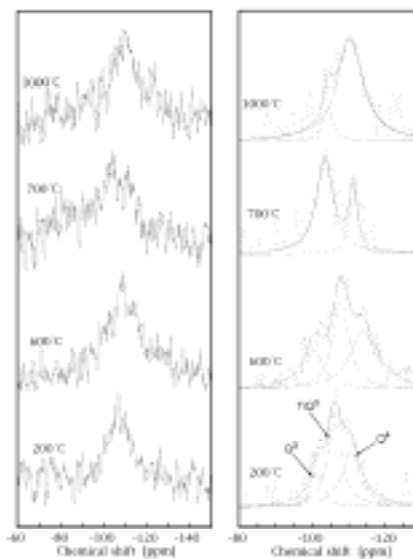


Table Siloxane units of CTS on pyrolysis^{a)}

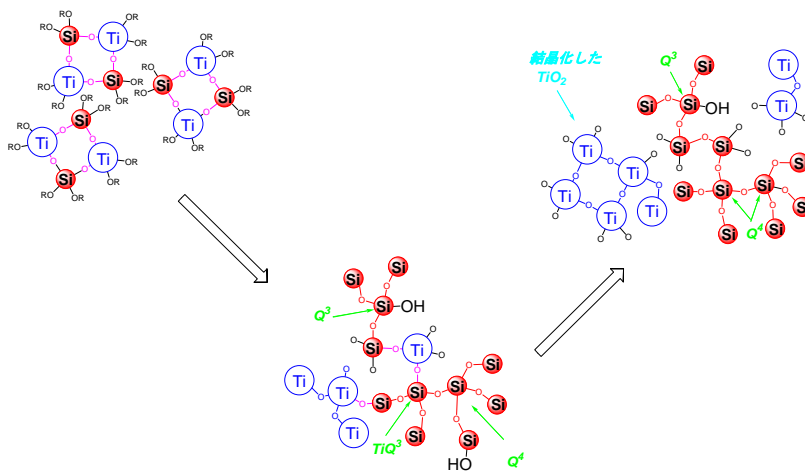
Temperature/ °C	Siloxane unit (%)		
	Q ³	TiQ ³	Q ⁴
200	16	46	38
600	20	39	41
700	75	0	25
1000	11	0	89

a) Calculated from ²⁹Si DD/MAS NMR after deconvolution.

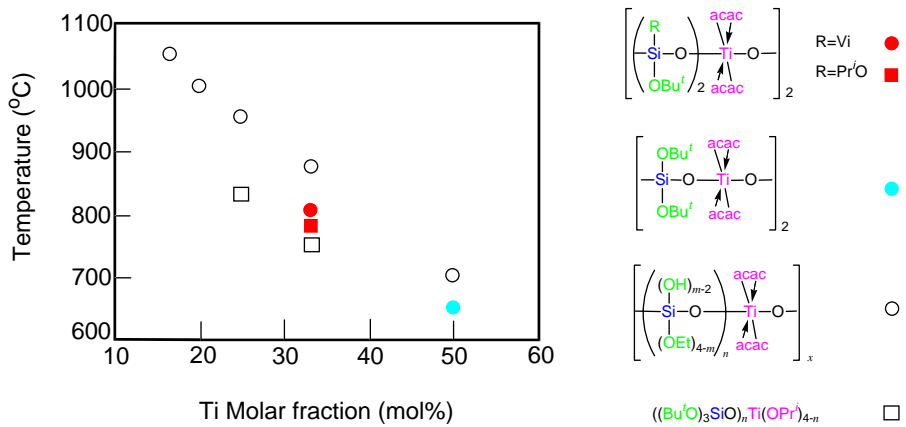


²⁹Si DD/MAS NMR spectra of CTS after heat-treatment

Deconvoluted ²⁹Si DD/MAS NMR spectra



Scheme 1 A model for the rearrangement of CTS on pyrolysis.

チタナシロキサン化合物のTiO₂(アナターズ晶)への結晶化温度

講演内容

1. アルコキシシランとチタン, ジルコニウムアルコキシド
2. チタナシロキサン, ジルコナシロキサン化合物
3. ポリジルコナシロキサン
4. ポリジルコノキサン

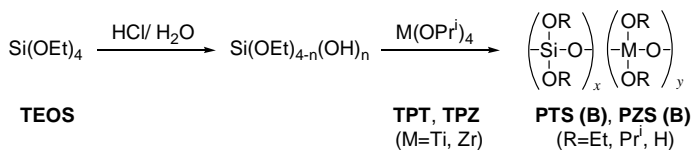
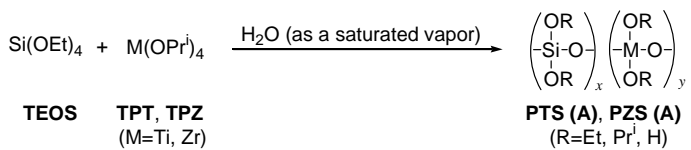


Table Preparation of APTS(A)^{a)} and APZS(A)^{b)}

No.	Polymetalla-siloxane	M	Time/ h	Yield/ %	Metal content			M_n ^{d)}
					Si/%	M/%	Si/M ^{c)}	
1	APTS(A)	Ti	48	36.3	6.03	14.8	0.44	3900
2			72	62.1	9.91	18.7	0.90	3700
3			96	80.2	10.3	16.7	1.05	3500
4			128	79.2	10.2	17.5	1.00	3500
5	APZS(A)	Zr	10	- ^{e)}				
6			20	9.8	0.92	19.3	0.15	1800
7			30	73.1	6.22	24.6	0.82	2900
8			35	87.5	6.64	24.9	0.86	3300
9			40	90.6	7.85	25.2	1.01	3600
10			43	90.4	7.80	25.3	1.00	3600
11			45	- ^{f)}				

a) TEOS: 10.42 g (0.05 mol), TPT: 14.21 g (0.05 mol); temp.: 24 °C.

b) TEOS: 4.17 g (0.02 mol), TPZ: 7.75 g (0.02 mol); benzene: 10 mL; temp.: 40 °C.

c) Molar ratio. d) Measured by VPO. e) No precipitation. f) Gelled.

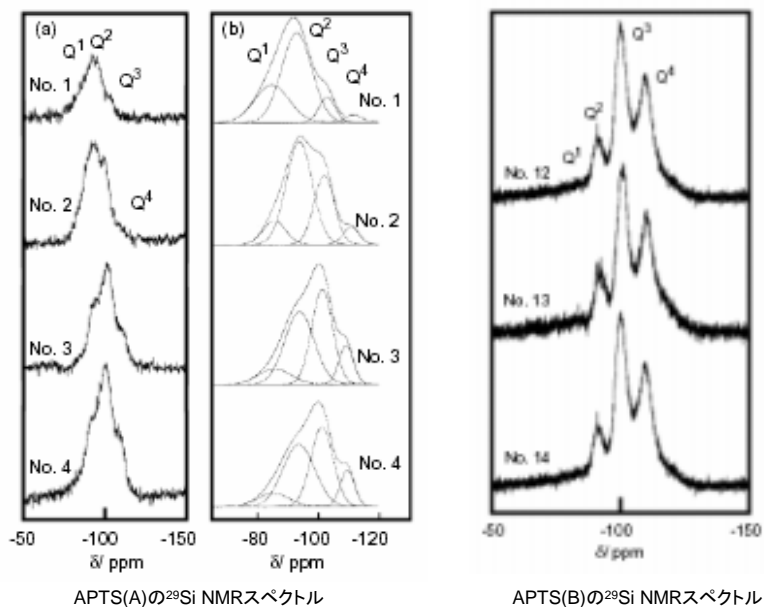
Table Preparation of APTS(B)^{a)} and APZS(B)^{b)}

No.	Polymetalla-siloxane	M	H ₂ O/TEOS Molar ratio	Yield/ %	Metal content			M_n ^{d)}
					Si/ %	M/ %	Si/M ^{c)}	
12	APTS(B)	Ti	2	79.8	7.06	15.0	0.82	2000
13			3	94.6	8.70	14.6	1.03	2200
14			4	91.6	9.11	14.0	1.12	2300
15	APZS(B)	Zr	2	60.2	5.51	22.4	0.80	2100
16			3	82.8	7.20	23.4	1.01	2400
17			4	85.4	7.96	23.4	1.10	2900

a) TEOS: 4.17 g (0.02 mol), TPT: 5.68 g (0.02 mol); ethanol: 40 mL; 2-propanol: 20 mL; HCl/TEOS molar ratio: 0.1.

b) TEOS: 4.17 g (0.02 mol), TPZ: 7.75 g (0.02 mol); ethanol: 100 mL; THF: 40 mL; HCl/TEOS molar ratio: 0.1.

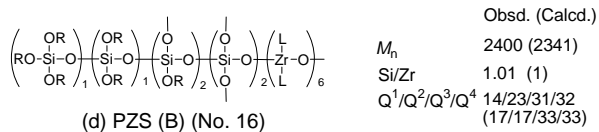
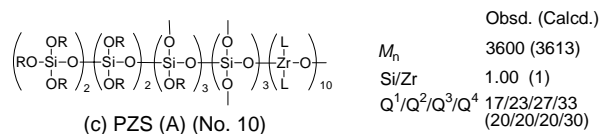
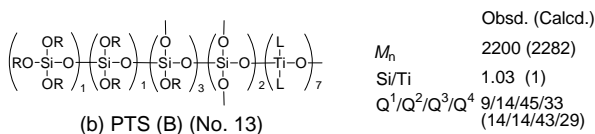
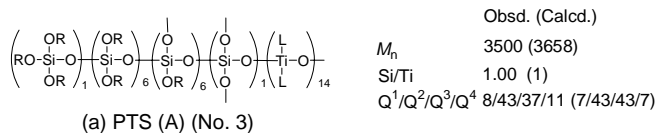
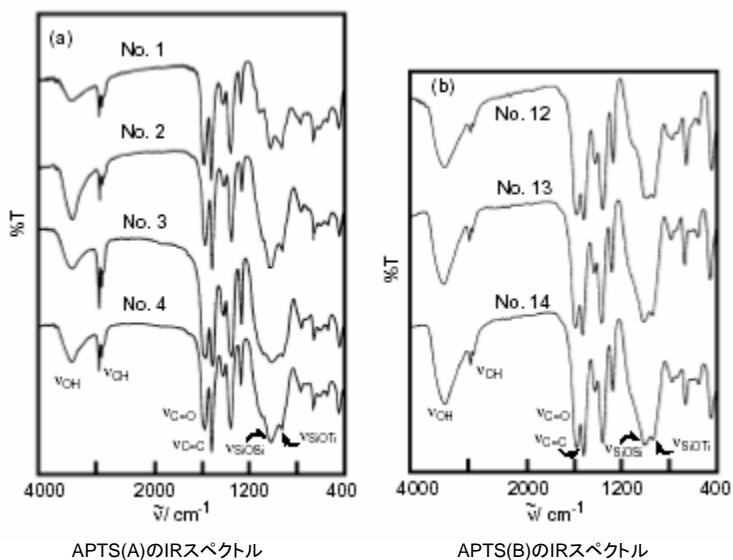
c) Molar ratio. d) Measured by VPO. e) No precipitation. f) Gelled.

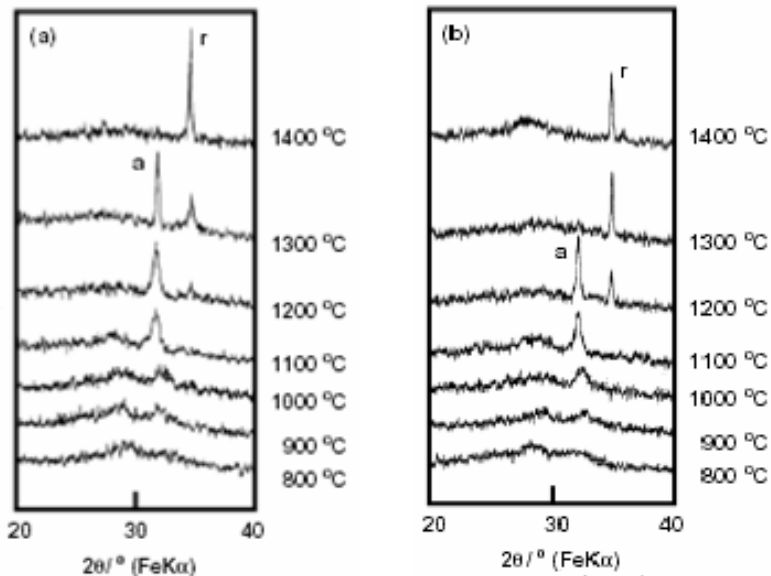
Table 3 Relative ratio^{a)} of peaks Qⁿ of polymetallasiloxanes

No.	Polymetallasiloxane	Percentage of silicon units ^{b)}			
		Q ¹	Q ²	Q ³	Q ⁴
1	APTS(A)	27	62	9	1
2		8	58	31	4
3		8	43	37	11
4		9	46	36	9
7	APZS(A)	21	39	28	12
8		20	28	29	23
9		19	24	26	31
10		17	23	27	33
12	APTS(B)	13	17	41	29
13		9	14	45	33
14		8	15	41	36
15	APZS(B)	15	22	34	29
16		14	23	31	32
17		7	19	34	40

a) Estimated from the results of ²⁹Si NMR spectra

b) A symbol Qⁿ denotes the microstructure of silicon atom as $\text{Si}(\text{OSi})_n(\text{OR})_{4-n}$.





APTS(A) No.3を焼成したときのX線回折図

APTS(B) No.13を焼成したときのX線回折図

Table Crystal form^{a)} and crystalline size^{b)} of APTS(A) for Nos. 1-3 and APTS(B) for Nos. 12-14 on heat treatment

Temp./ °C	Crystal form and crystalline size/ nm					
	APTS(A)			APTS(B)		
	No. 1	No. 2	No. 3	No. 12	No. 13	No. 14
600	-	-	-	-	-	-
650	A (36)	-	-	-	-	-
700	A (39)	-	-	-	-	-
750		A (36)	-	A (45)	A (43)	-
800	A (46)	A (41)	-	A (46)	A (47)	-
850			A (41)			A (38)
900	A (80)	A (55)	A (49)	A (91)	A (66)	A (61)
1000	A (125), R	A (110)	A (65)	A (106)	A (91)	A (84)
1100	A (241), R	A (202), R	A (144)	A (212), R	A (198), R	A (161)
1200		R A (234), R	A (271), R	A (297), R	A (372), R	A (223), R
1300		R	A (305), R	R	A (411), R	A (440), R
1400		R	R	R	R	R

a) -: Amorphous, A: anatase form of TiO₂, R: rutile form of TiO₂.

b) Represented in the parentheses. Calculated from Scherrer's equation.

Table Crystal form^{a)} and crystalline size^{b)} of APZS(A) for Nos. 7, 8, and 10 and APZS(B) for Nos. 15-17 on heat treatment

Temp./ °C	Crystal form and crystalline size/ nm					
	APZS(A)			APZS(B)		
	No. 7	No. 8	No. 10	No. 15	No. 16	No. 17
400	-	-	-	-	-	-
450	-	-	-	T (43)	-	-
500	-	-	-	T (46)	-	-
600	T (56)	-	-	T (56)	-	-
700	T (62)	-	-	T (70)	-	-
750		T (35)	-		T (46)	-
800	T (70)	T (37)	T (32)	T (83)	T (55)	T (49)
1000	T (74)	T (63)	T (62)	T (101)	T (70)	T (56)
1100	T (112)	T (96)	T (86)	T (112)	T (86)	T (82)
1200	T (223)	T (186)	T (159)	T (207)	T (169)	T (159)

a) -: Amorphous, T: tetragonal ZrO₂.

b) Represented in the parentheses. Calculated from Scherrer's equation.

講演内容

1. アルコキシシランとチタン, ジルコニウムアルコキシド
2. チタナシロキサン, ジルコナシロキサン化合物
3. ポリジルコナシロキサン
4. **ポリジルコノキサン**

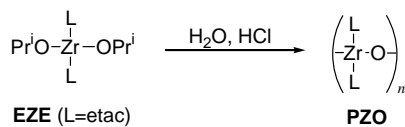
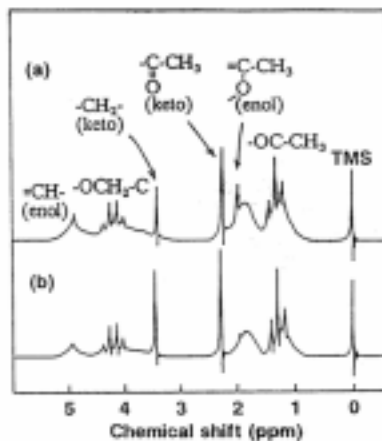


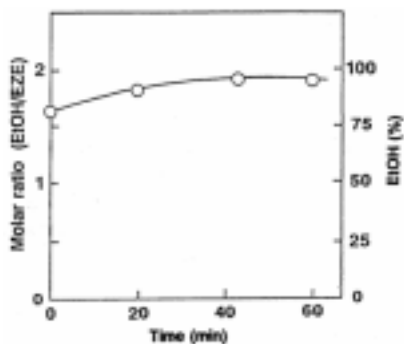
Table Hydrolysis condition for EZP and spinnability of concentrated PZO methanol solution.

Molar ratio		Time/ h	Spinnability ^{b)/} cm
H ₂ O/EZP	HCl/EZP		
1.0	0.1	1	70
1.5	0.1	1	80
2.0	0.1	1	55
1.0	0.2	1	50
1.5	0.2	1	120
1.5	0.2	8	100
2.0	0.2	1	70
2.5	0.2	1	0

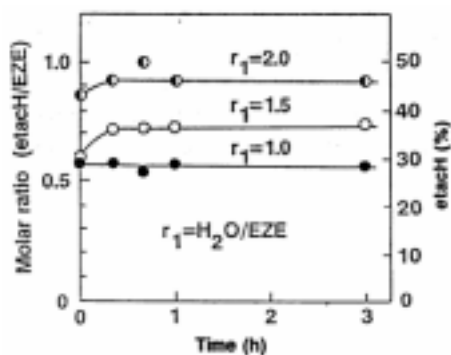
a) Concentrated methanol solution (84 wt%);
Hydrolysis of EZP was carried out in MeOH.



¹H NMR spectra of PZO in CCl₄ (a) and CDCl₃ (b)



Results of the determination of EtOH formed
During the hydrolysis of EZE.



Results of the determination of etach formed
During the hydrolysis of EZE.

Table Analytical data for PZO and the hydrolysis products of EZE.

	Observed Value
Ethanol formed by hydrolysis/ mol	1.9 ^{a)}
etacH formed by hydrolysis/ mol	0.72 ^{a)}
PZO Molecular weight (Mn) by VPO	820
Zr content/ %	32.3 ^{b)}
etac/Zr molar ratio	1.1 ^{c)}
OH/etac molar ratio	0.6 ^{d)}

a) Against one mole equivalent of EZE.

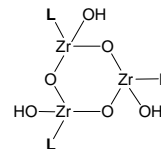
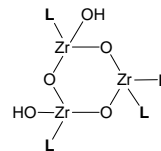
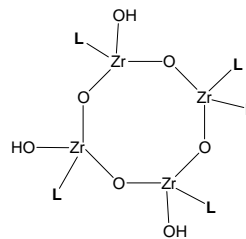
b) Analysis: C 28.4 %, H 4.0 %.

c) $\text{etac/Zr} = \text{C/Zr} = (28.4/12.0/6)/(32.3/91.2) = 1.1$

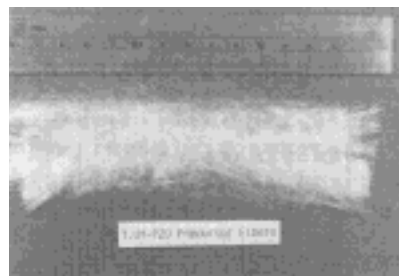
d) Observed from the proton ratio of silylates by NMR.

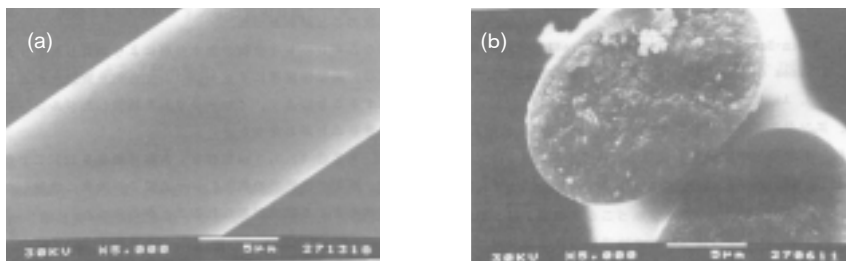
Table Analytical data for the estimated structures of PZO.^{a)}

	Compositions				MW	Elemental Analysis/ %			Molar ratio	
	x	y	z	w		C	H	Zr	etac/Zr	OH/etac
Observed					870	28.4	4.0	32.3	1.1	0.6
	4	3	5	4	1126	32.0	4.3	32.4	1.25	0.6
Calcd.	3	2	4	3	872	33.0	4.4	31.4	1.33	0.5
	3	3	3	3	760	28.4	4.0	36.0	1.0	1.0

a) Formula: $\text{Zr}_x(\text{OH})_y(\text{etac})_z\text{O}_w$ 

乾式紡糸装置

水蒸気処理後の前駆体繊維
(3.0Y-PZO:Y₂O₃を3%含有)



1200°Cで1h焼成して調製した3.0Y-PZO繊維の表面(a)と断面(b)のSEM写真

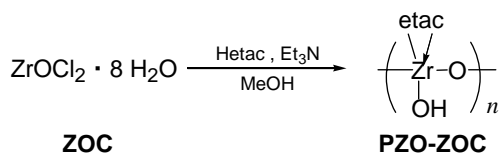


Table Results on the preparation of PZO-ZOC

Yield / %	State	Metal analysis ^{a)} / % (calcd.)
70.6	White powder	37.8 (36.0)

a) Determined by ICP.

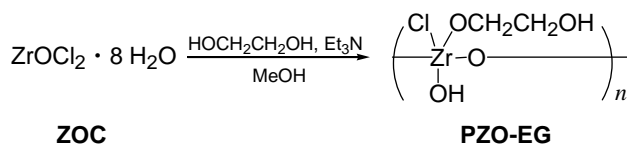


Table Results on the preparation of PZO-EG

Yield / %	State	Metal analysis ^{a)} / % (calcd.)
95.2	White powder	41.9 (41.2)

a) Determined by ICP.